Journal of Medical Imaging

MedicalImaging.SPIEDigitalLibrary.org

Automated contour tracking and trajectory classification of pelvic organs on dynamic MRI

Iman Nekooeimehr
Susana Lai-Yuen
Paul Bao
Alfredo Weitzenfeld
Stuart Hart

SPIE.

Iman Nekooeimehr, Susana Lai-Yuen, Paul Bao, Alfredo Weitzenfeld, Stuart Hart, "Automated contour tracking and trajectory classification of pelvic organs on dynamic MRI," *J. Med. Imag.* **5**(1), 014008 (2018), doi: 10.1117/1.JMI.5.1.014008.

Automated contour tracking and trajectory classification of pelvic organs on dynamic MRI

Iman Nekooeimehr,[a] Susana Lai-Yuen,[b,*] Paul Bao,[c] Alfredo Weitzenfeld,[c] and Stuart Hart[d,e]
[a]Revenue Analytics, Atlanta, Georgia, United States
[b]University of South Florida, Department of Industrial and Management Systems Engineering, Tampa, Florida, United States
[c]University of South Florida, Department of Computer Science and Engineering, Tampa, Florida, United States
[d]University of South Florida, Department of Obstetrics and Gynecology, Tampa, Florida, United States
[e]Medtronic, Tampa, Florida, United States

Abstract. A method is presented to automatically track and segment pelvic organs on dynamic magnetic resonance imaging (MRI) followed by multiple-object trajectory classification to improve understanding of pelvic organ prolapse (POP). POP is a major health problem in women where pelvic floor organs fall from their normal position and bulge into the vagina. Dynamic MRI is presently used to analyze the organs' movements, providing complementary support for clinical examination. However, there is currently no automated or quantitative approach to measure the movement of the pelvic organs and their correlation with the severity of prolapse. In the proposed method, organs are first tracked and segmented using particle filters and *k*-means clustering with prior information. Then, the trajectories of the pelvic organs are modeled using a coupled switched hidden Markov model to classify the severity of POP. Results demonstrate that the presented method can automatically track and segment pelvic organs with a Dice similarity index above 78% and Hausdorff distance of <5.2 mm for 94 tested cases while demonstrating correlation between organ movement and POP. This work aims to enable automatic tracking and analysis of multiple deformable structures from images to improve understanding of medical disorders. [DOI: 10.1117/1.JMI.5.1.014008]

Keywords: contour tracking; trajectory classification; magnetic resonance imaging; pelvic organs.

Paper 17308R received Oct. 13, 2017; accepted for publication Mar. 12, 2018; published online Mar. 30, 2018.

1 Introduction

Pelvic organ prolapse (POP) is a major health problem that affects up to 30% to 50% of women[1] with direct costs of about $1 billion per year.[2] POP is a herniation of the female pelvic floor organs (bladder, uterus, small bowel, and rectum) into the vagina. This condition can cause significant health implications, including a bothersome vaginal bulge, and incomplete bowel and bladder emptying. However, very little is known about the risk factors of POP even though it is one of the most common reasons for gynecological surgery according to the National Center for Health Statistics.[3] This makes POP a common but poorly understood condition. Currently, POP is diagnosed through clinical examination using the POP quantification (POP-Q) system, which is a standardized method for quantifying and staging POP.[4] However, it only allows partial assessment of the pelvic floor anatomy making it difficult to observe pelvic organ descent dynamics in all compartments that could improve understanding of POP.[5] Better understanding of the prolapsing pelvic organs and their movement could be clinically important for recommending appropriate treatment and POP repair surgery, which currently has a reported high failure rate of 30%.[6]

To better understand pelvic organ dynamics, data obtained through dynamic magnetic resonance imaging (MRI) of the pelvic floor have been increasingly studied and used for POP assessment.[7–10] Dynamic MRI of the pelvic floor consists of a sequence of two-dimensional MRI images taken along the midsagittal plane during straining maneuvers of the patient that begin from rest to maximal straining as shown in Fig. 1. It can be observed from the figure that pelvic organs, such as the bladder, rectum, and uterus, move and deform significantly with respect to bony structures. This enables observation of pelvic organ descent dynamics in all compartments simultaneously to complement clinical examination in the assessment of POP.[11]

Various approaches have been proposed to assess POP using dynamic MRI and its correlation to clinical examination outcomes. The most common approach is to manually identify reference lines and extract corresponding measurements from the maximum strain frame only. Three of the most widely used reference lines are the pubococcygeal line (PCL),[12] H-line,[13] and midpubic line (MPL).[12] In addition, dynamic MRI has been used to analyze the displacement of the pelvic organs. Some studies have indicated some association between the movement of the pelvic organs' centroids and POP.[14,15] However, these studies localized and segmented the organs manually or semiautomatically. There is currently no automated or quantitative approach to measure multiple pelvic organ movement and their correlation with prolapse.

Some of the challenges of automating the analysis of multiple organ movements on dynamic MRI are as follows: (1) many of the frames from the dynamic MRI sequence do not provide additional information as the movement of pelvic organs during straining maneuvers is fast and captured in only a few frames, (2) within the few frames that capture organ movement, organs sometimes move significantly among consecutive frames so their boundaries do not overlap across the frames, and (3) the

*Address all correspondence to: Susana Lai-Yuen, E-mail: laiyuen@usf.edu

2329-4302/2018/$25.00 © 2018 SPIE

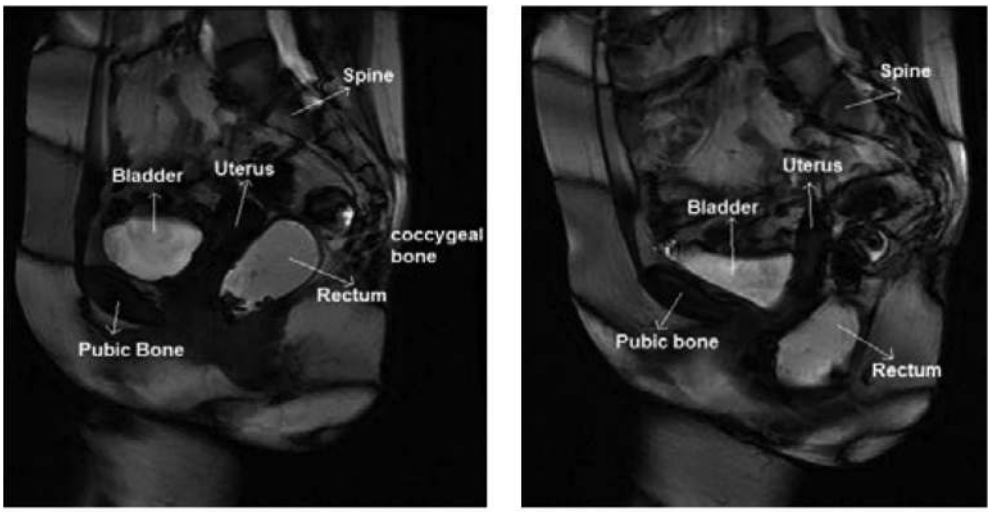

Fig. 1 Midsagittal dynamic MRI: frame at (a) rest and (b) maximum strain.

trajectories of pelvic organs need to be modeled together to capture the interactions among the organs.

In this research, a model is presented to automatically track, segment, and analyze multiple pelvic organ movement in dynamic MRI, and a coupled switched hidden Markov model (CSHMM) is proposed to analyze the movement and interactions of the organs. The outcome of this model aims to provide better understanding of POP through organ movement analysis to potentially improve its diagnosis and treatment. A contour tracking method is proposed to track and segment multiple pelvic organs from a sequence of dynamic MRI images. In the first stage, the proposed method tracks the pelvic organs over the frame sequence to generate initial contours that are used for subsequent organ segmentation and to identify those frames that contain changes in organ movement. This removes uninformative frames to avoid unnecessary segmentation and tracking. In the second stage, pelvic organs are segmented using the contours generated in the first stage. Finally, a CSHMM is proposed as a dynamic Bayesian model to analyze multiple trajectories and their interactions. This model aims to analyze multiple organs movement and define MRI-based features to complement clinical examination for POP assessment.

2 Related Work

Extensive surveys for object tracking can be found in Refs. 16–18. Tracking deformable objects is more challenging because the object may go through changes in size, shape, and texture during the image sequence making it difficult and sometimes impossible to track. For trajectory classification, reviews can be found in the work by Morris and Trivedi[19] and Aggarwal and Ryoo.[20]

Dynamic models have been proposed to take into account the temporal ordering of the trajectories. A standard hidden Markov model (HMM) can be used to model multiple-objects trajectories, which results in multidimensional state states and observation spaces.[21] A multiobservation HMM was suggested, in which the observation space is factorized by defining multiple observation variables in each time interval.[22] A parallel HMM[23] was proposed, where both space state and observation states are factorized. A distributed multidimensional HMM was proposed in Ref. 24, which first models the trajectories as a noncausal, multidimensional HMM and then distributes the noncausal model into multiple-distributed causal HMMs. Previous approaches either do not consider interactions among objects or require large computations.

While there has been extensive research on the dynamics of body organs, such as brain,[25] heart,[26] and lungs,[27] few groups have conducted research on the movement and deformation of soft tissues in the pelvic area. In Ref. 28, landmarks are tracked over the boundary of pelvic organs during strain for prolapse analysis. Another work focused on generating biomechanical models to simulate pelvic organ movement.[29] A finite-element-based numerical simulation was presented in Ref. 30 to study the effects of vaginal delivery on the pelvic floor. However, these works segmented the organs using manual or semiautomatic approaches.

Current contour tracking or boundary-based object tracking methods require manual localization of the objects to be segmented. They also rely on the assumption that the boundaries of the objects to be tracked and segmented are overlapping in consecutive frames. The dynamic MRI taken for POP contains multiple frames with no changes that do not provide any additional information. Thus, these uninformative frames need to be identified and removed to avoid unnecessary segmentation. Moreover, the boundaries of the organs do not always overlap in consecutive frames.

3 Methodology

The proposed method to automatically track, segment, and analyze the movement of pelvic organs is described in this section and shown in Fig. 2. The process starts with the data collection followed by a contour tracking method for automated tracking and segmentation of pelvic organs using prior information. Finally, the pelvic organ trajectories are analyzed using a proposed CSHMM that extends and solves the concept of switched HMM[31] for multiple trajectories.

3.1 *Data Acquisition*

A representative clinical dataset of 94 cases with dynamic MRI was used in this study. The distribution for the three types of prolapse, anterior (for bladder), apical (for uterus), and posterior

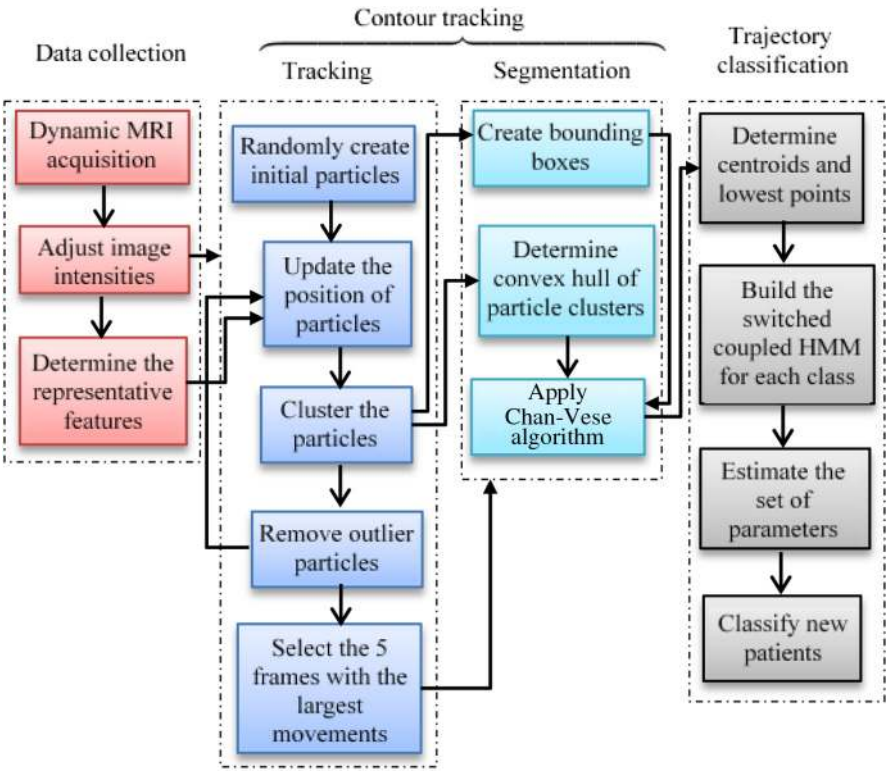

Fig. 2 Overview of the proposed predictive model.

(for rectum), is shown in Table 1. The Institutional Review Board at the University of South Florida considered the study exempt since all protected health information was previously removed from the clinical and MRI data before being collected from a database for this study. MR imaging was taken on a 3-Tesla GE system (General Electric Company, GE Healthcare, Buckinghamshire, United Kingdom) using an 8-channel torso phased-array coil with the patient in a modified dorsal lithotomy position. Prior to imaging, 60 ml of ultrasound gel was placed in the rectum for improved visualization. Dynamic MRI of the pelvis was performed using a T2-weighted single-shot turbo spin-echo sequence in the midsagittal plane with a temporal resolution of 2 s (field of view 300×300 mm^2, slice thickness 3 mm, TR/TE 2000/75 ms, 20 image sequences, and in-plane resolution of 1.6×1.6 mm^2). Patients were coached, prior to imaging, on performance of an adequate valsalva maneuver.

Each patient has 20 frames showing the pelvic floor structures from rest to maximum strain. The image data have been preprocessed and deidentified. For the ground truth, each patient in the dataset was previously examined clinically using the POP-Q system resulting in a POP stage assignment that ranges from 0 to 4, where 4 is the highest level of POP severity. A stage was assigned for each of the three types of prolapse resulting in three separate stages for the patient (a patient can have one or multiple types of prolapse). The current study was designed as a two-class classification problem to differentiate cases of low and high stages of POP. In this study, low prolapse was defined as stage 0 or 1, and high prolapse was defined as stage 2, 3, or 4. The aim is to identify patients who most likely require repair surgery (high prolapse) versus patients who do not (low prolapse) based on pelvic organ movement. Thus, this study aims to analyze the relationship between multiple pelvic organ movement and severity of prolapse to improve understanding of the condition, and potentially improve POP diagnosis and treatment by complementing clinical examination.

Before analyzing the MRI data, the images are normalized to improve the contrast of the input images by stretching the range of intensity values. Then, a training set is selected from the dataset to analyze and extract a representative set of intensity and texture features R for the bladder and rectum. The texture features include the range, standard deviation, and entropy. The uterus, although also a pelvic organ, is not considered in this work as some cases in our dataset belong to patients whose uterus has been surgically removed.

Table 1 Composition of the dataset based on POP severity for the three types of POP.

POP type	Low prolapse	High prolapse
Anterior	34	60
Apical	78	16
Posterior	26	68

3.2 *Automated Tracking and Segmentation of Pelvic Organs Using Prior Information*

In the first stage of the proposed method, the bladder and rectum are tracked using an adapted particle filter approach with prior information. This information consists of the relative locations and common movement directions of the pelvic organs. The following prior information has been incorporated in the particle filter tracking and is explained in more detail throughout this section:

- No part of the bladder and rectum is located on the top quartile of the images.
- The pelvic organs tend to move down or to the right during dynamic MRI.
- The bladder is always on the left side of the image while the rectum is on the right side.

This prior information is used to improve the generation, updating, and resampling of the particles. For example, since no part of bladder and rectum is located in the top quartile of the images, particles are not generated on this quartile to improve particle tracking.

Then, for each frame, the following steps are performed:

1. Update the position of the particles by assuming a proper velocity. We assume uniform linear motion for the bladder and rectum, and use prior information on their common movement directions to improve the tracking results. This is achieved by updating the particles using the linear velocity and imposing higher chances that a particle moves down or to the right.

2. Calculate the likelihood of particles $L^{(k)}$. For each particle k, we measure how close its features q_k are from R, where σ is the standard deviation of $(q_k - R)$

$$L^{(k)} = \frac{1}{\sqrt{2\pi\sigma}} \exp\left(-\frac{(q_k - R)^2}{2o^2}\right).$$

3. Resample the particles with replacement according to their likelihood, where P^k is the likelihood of the k'th particle and N is the number of particles

$$P^{(k)} = \frac{L^{(k)}}{\sum_{v=1}^{N} L^{(v)}}.$$

After resampling, for each frame, we use k-means to cluster the particles into two groups corresponding to each pelvic organ (bladder and rectum). Prior information on the relative location of the bladder and rectum in the image is incorporated to provide a better initialization for the k-means clustering. In particular, it is known that the bladder is always on the left side of the image while the rectum is on the right side. Therefore, the initial placement for the centers in k-means is based on this information to improve clustering of the two organs. Outlier particles are removed from each cluster using the Grubbs test,[32] because during the resampling there is a chance that some particles with low likelihood are selected. The Grubbs's test statistics of all particles to their corresponding center is measured based on their distance assuming they have normal distribution. Then, the ones that are statistically farther from the center at $\alpha = 0.05$ are identified as outliers and are eliminated.

Our analysis of the image dataset showed that for all cases only 3 to 5 frames out of the 20 frames provide information on changes in pelvic organ movement whereas the remaining frames show no pelvic organ movement. For this reason, segmentation is performed only on a representative set of five frames to avoid unnecessary segmentation on uninformative frames. In this work and for each case in the dataset, the movement of particles' centroids for bladder and rectum is measured over all the frames. Then, the five frames with the largest movement are selected as the representative frames.

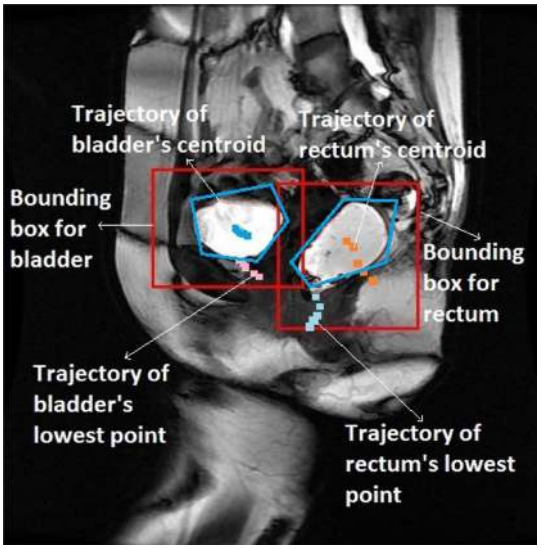

Fig. 3 Generated bounding box (red) and initial contour (blue) for bladder (left side) and rectum (right side) using their corresponding particles and four trajectories to be analyzed for each patient.

The resulting two clusters of particles are used to define a bounding box for each pelvic organ to constrain the search space during segmentation and significantly reduce the computational time. An initial adaptive contour is proposed for segmentation that is generated from the convex hull of each particle cluster. This provides a good initial contour to initialize the Chan–Vese contour segmentation algorithm[33] and automate the process. In contrast with the original Chan–Vese algorithm that requires an initial contour to be manually defined for each frame, our approach determines the initial contour for each frame automatically and adaptively using the convex hull of particles to identify the boundaries of the bladder and rectum. The generated bounding box and convex hull to initialize the segmentation algorithm are shown in Fig. 3.

3.3 *Multiple Pelvic Organs Trajectory Analysis*

From Sec. 3.2, the trajectory of the bladder's and rectum's centroids and lowest points are extracted. The lowest points are considered, because they are of clinical interest to determine the stage (or severity) of prolapse. This leads to four trajectories for each patient as can be seen in Fig. 3. A method called CSHMM is proposed to capture the interactions among the four trajectories to classify the severity of POP.

In this work, patients are to be classified into two classes: high severity of prolapse (class $+1$) and low severity of prolapse (class -1), so the set of output variable is $c \in \{+1, -1\}$. For each patient i in class c, there exist four trajectories $l \in \{1, 2, 3, 4\}$ with the sequence of positions $x_l = (x_{1l}, \ldots, x_{5l})$ where $x_{lt} \in \Re^2$. CSHMM is a generative model; hence, a separate model should be made for the examples of each class. As shown in Fig. 4, the state of each trajectory at time t depends on its own state at time $t-1$, its observation at time t and on the states of other trajectories at time $t-1$.

We consider the observed variables as the set of the relative movement $\{d_{lt} = (x_{l,t+1} - x_{l,t}), l = 1,2,3,4; t = 1,2,3,4\}$ of the four trajectories rather than their absolute positions $X = \{x_l, l = 1,2,3,4\}$ because we want to study the movements of the

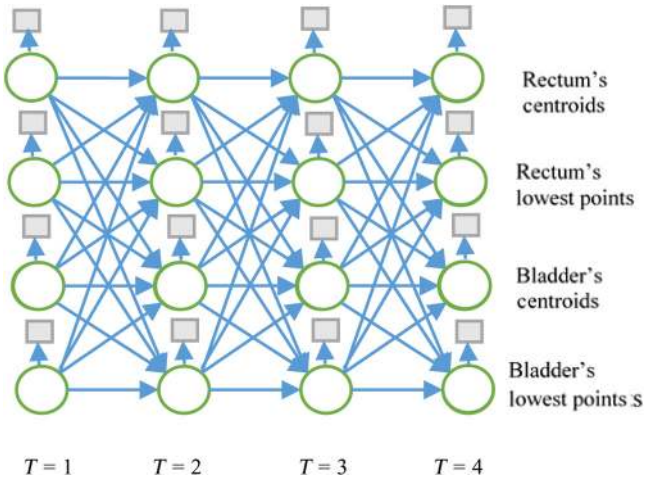

Fig. 4 Proposed CSHMM.

organs. As shown in Fig. 5, the hidden states in our model are "stopped," "moving up," "moving down-right," "moving down," and "moving down-left."

Given the observed feature vector $\{d_l = (d_{l1}, \ldots, d_{l4}), l = 1, 2, 3, 4\}$ and the corresponding set of hidden state $\{h_l = (h_{l1}, \ldots, h_{l4}), l = 1, 2, 3, 4\}$, the task is to estimate the set of parameters $\gamma_c = (\Pi_c, \theta_c, A_c)$ for each class c. $\Pi_c = \{\pi_c(S_1, \ldots, S_4), S_l = 1, \ldots, N, l = 1, 2, 3, 4\}$ are the initial probabilities for the states, given that each state can take N different values. θ_c is the set of parameters for the Gaussian distribution, including the mean $\mu_{(S_1,\ldots,S_4)}$ and the variance $\Sigma_{(S_1,\ldots,S_4)}$, and A_c is the state transition probabilities. In contrast to Ref. 31, in which first the Gaussian parameters θ_c are estimated and then (Π_c, A_c) are estimated separately, in our method, all the parameters are determined simultaneously resulting in better estimation of the parameters at the expense of higher computational time.

After building a model for each type of prolapse, the next step is to classify new cases having a set of four observed trajectories. The "maximum a posteriori" rule is being used for this purpose:

$$c = \arg\max_c\{p(x|c)p(c)\}$$
$$= \arg\max_c\{p(x|\hat{\Pi}_c, \hat{\theta}_c, \hat{A}_c)p(c)\},$$

in which the $p(x|\hat{\Pi}_c, \hat{\theta}_c, \hat{A}_c)$ is the log likelihood of the most probable explanation (mpe) of example x using the model for class c, and $p(c)$ is the "a priori" probability of the class c. In our experiments, we set $p(c)$ equal to the proportion of each class in the dataset. Hence, we set $p(c = +1) = 0.34$ and $p(c = -1) = 0.66$. We also used the Viterbi algorithm[34] to find the mpe and likelihood of each new patient for each model.

4 Results

The proposed model was tested on 94 cases, which were manually segmented by an expert as the ground truth. Tracking and segmentation results were evaluated using Dice similarity index (DSI) and Hausdorff distance to quantify the degree of overlap and their spatial distance among objects, respectively. DSI[35] was used as a quantitative measure of the overlap between our method's segmentations and the ground truth segmentation. The value of DSI ranges from 0 to 1, where 0 indicates no intersection between the ground truth and automatically segmented regions and 1 indicates a complete overlap between the two segmentations. Hausdorff distance[36] is a measure to estimate the spatial distance between two sets of points. The smaller

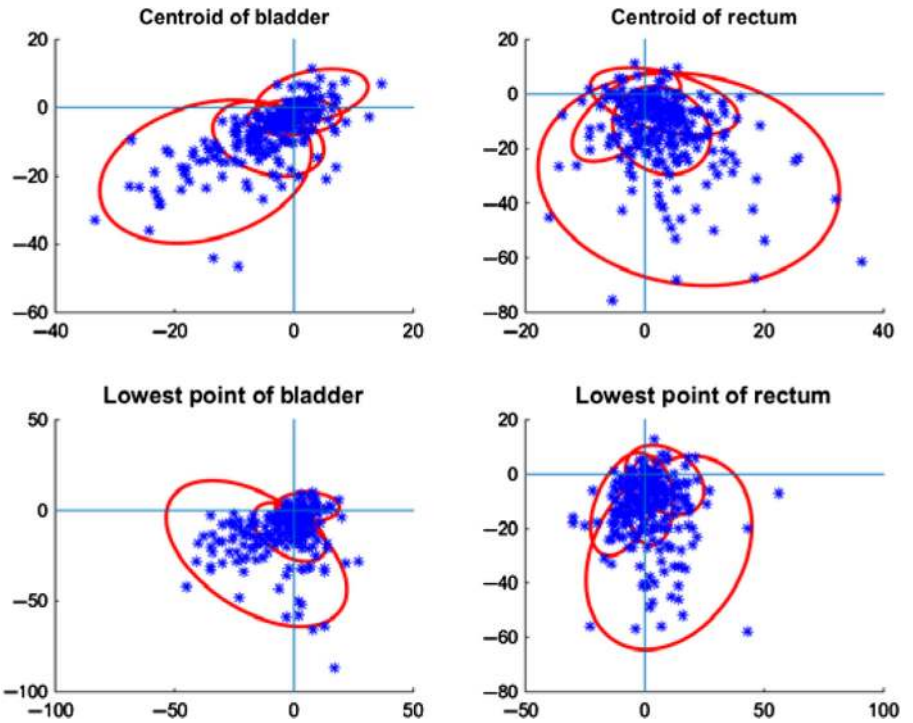

Fig. 5 The scatterplot of trajectories' displacement. Each eclipse refers to the Gaussian distribution of the hidden states. The hidden states include "stopped," "moving up," "moving down-right," "moving down," and "moving down-left."

Table 2 Summary statistics for the total displacement (in mm) of the lowest points for the bladder and rectum.

POP type	Total ($n = 94$)	Low prolapse	High prolapse	P-value
Anterior	37.049 ± 23.375	27.446 ± 15.429	42.491 ± 25.394	0.0023*
Posterior	39.749 ± 23.375	34.983 ± 24.016	41.5718 ± 19.557	0.1741

*$p < 0.05$.

the distance implies the closeness of the two sets and better segmentation.

For each patient, the DSI and Hausdorff distance for the five frames were calculated and averaged. Then the averaged DSI for all the patients was averaged over the 94 patients. Results indicate that the proposed method is able to automatically track and segment bladder with a DSI of 0.8957 ± 0.0146 and Hausdorff distance of 4.1567 ± 0.506 mm. The DSI for rectum is 0.6720 ± 0.0654 and the Hausdorff distance is 6.3262 ± 0.5330 mm.

To determine whether there is a relationship among pelvic organs movement on dynamic MRI with the severity of prolapse, the maximum displacement of the organs' lowest point from rest to maximum strain was analyzed. The mean and standard deviation of this displacement were determined for the total study population and compared with the two classes of prolapse (low severity and high severity) as shown in Table 2. The statistical significance of the maximum displacement difference between the two classes was measured using a two-sided t-test. Alpha $= 0.05$ was used to accept or reject whether there exists a difference between the two classes for each organ. As can be seen from Table 2, at $\alpha = 0.05$, the difference is significant for anterior prolapse. On the other hand, although on average the rectum was shown to move more for the case of high severity of prolapse, the difference in displacement from rest to maximum strain was not found to be significant for posterior prolapse. Therefore, we can conclude that for the case of anterior prolapse, large bladder displacement observed on MRI from rest to maximum strain is related to high severity of prolapse. However, a similar conclusion cannot be made for posterior prolapse.

In addition, it was studied whether there exists any correlation between the lowest point's largest displacement of the bladder and rectum on MRI from rest to maximum strain. Figure 6 shows the displacement of the bladder on the y-axis and the displacement of the rectum on the x-axis. Kendall's tau for the correlation was 0.3636 and the p-value was 2.2113×10^{-07}. The Pearson's correlation coefficient was 0.3905 and the p-value was 9.9720×10^{-05}. Thus, at $\alpha = 0.05$, we can conclude that there exists enough evidence that the maximum displacement of the bladder and rectum is correlated. This indicates that a large bladder displacement tends to also present with high rectum displacement and vice versa. These results confirm the importance of considering the interactions of pelvic organs to improve understanding of the condition.

The proposed CSHMM was compared with single trajectory classification, in which one single trajectory (the centroids) represents each organ and the interactions of the organs are not considered. In this case, the trajectory of the rectum's centroids is used to predict the severity of posterior prolapse, whereas the trajectory of bladder's centroid is used to predict the severity of anterior prolapse. Given that the dataset contains some patients whose uterus has been surgically removed, it was not possible to track and segment the uterus to perform the single trajectory analysis for apical prolapse. Instead, for the multiple trajectory analysis, the trajectories of the bladder and rectum were used to determine the severity of apical prolapse. The proposed CSHMM is also compared with two commonly used manual MRI-based measurements: (1) PCL and (2) MPL. PCL is defined as the line connecting the inferior rim of the pubic bone and the last visible coccygeal line. MPL is defined as the line drawn through the longitudinal axis of the pubic bone and passing through its midequatorial point. These measurements were obtained for all the cases in the dataset by an expert radiologist and were converted to stages of prolapse using the standard criteria described in Ref. 37.

Leave-one-out cross validation was used to measure the performance of the prediction model in terms of accuracy and F-measure. In leave-one-out cross validation, all but one of the examples from the dataset are used for training the model, and the remaining example is used for testing the model. This process is repeated for each of the examples in the dataset to predict if the example has high severity of prolapse or not. The prediction for each example is compared with the POP-Q measurement of each example to obtain the accuracy and the F-measure of all 94 examples. F-measure is the weighted average of recall and precision, and a suitable performance metric when the dataset is imbalanced, such as our dataset. Precision measures the exactness of our prediction model, that is, the number of patients who were predicted correctly with high prolapse from the model's positive predictions. Recall measures the completeness of our prediction model as the number of patients with high severity of prolapse was predicted correctly from the sample. The experiments were repeated three times to report the average in order to alleviate the randomness effects on the results. The comparison between MPL, PCL, and our method for the three types of prolapse is shown in Table 3. The N/A values in Table 3

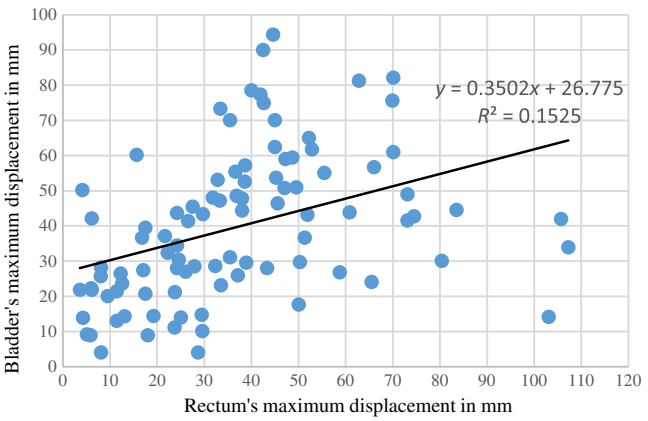

Fig. 6 Correlation of rectum's maximum displacement and bladder's maximum displacement.

Table 3 Results comparing our proposed CSHMM with commonly used manual MRI-based measurements to predict severity of POP. Best results are indicated in bold.

POP type	Measurement	PCL	MPL	Single trajectory	Proposed method
Anterior	Accuracy	0.3589	0.5598	**0.6596**	0.6277
	F-measure	0.3524	0.6309	0.4667	**0.6317**
Apical	Accuracy	0.7321	0.7608	N/A	**0.8191**
	F-measure	0.8427	0.8512	N/A	**0.8957**
Posterior	Accuracy	0.4354	0.5502	0.6596	**0.6702**
	F-measure	0.4327	**0.4891**	0.3846	0.4364

are for the single trajectory analysis of apical posterior, since the uterus was not tracked and segmented.

5 Discussion

As seen in the results, the proposed model provides greater accuracy compared to the current manual MRI-based measurements (PCL and MPL) for all types of prolapse. In terms of *F*-measure, the proposed method shows better results for both MPL and PCL for anterior and apical prolapse, respectively, but not for posterior prolapse. Also, in agreement with the results in Ref. 37 and as a secondary conclusion, MPL measurements work better than PCL for the three types of prolapse in all our 94 patients. The proposed method aims to complement clinical examination (POP-Q) and enhances our understanding of POP through an automated and quantitative MRI-based approach for organ movement analysis. In particular, the proposed method provides a model based on the trajectories and interactions of multiple pelvic organs on dynamic MRI compared to current static measurements (PCL and MPL) that are extracted only at the maximum strain frame.

Deep learning approaches, such as recurrent neural networks and long short-term memory, have been presented for learning temporal dynamics. However, HMMs are simpler, more interpretable, better suited for short temporal horizons, and require less training data. For these reasons, we used an HMM approach as our dataset is not very large, the time for organ movement analysis is short, and model interpretability is very important for our application.

Although the proposed method correctly segmented the pelvic organs in our dataset, segmentation challenges may present in cases where gas accumulates inside the rectum during image acquisition. This can be observed in the segmentation results for the rectum. As future work, additional data will be collected and processed to perform experiments and generalize the method on a larger dataset and to analyze the impact of the uterus' trajectory on classification.

6 Conclusions

In this paper, an automatic method was presented to track, segment, and analyze the trajectories of pelvic organs on dynamic MRI. A modified particle filter approach was designed by incorporating prior information and clustering to track the pelvic organs automatically. An adaptive initial contour for segmentation using the convex hull of the particle clusters was proposed to automatically remove uninformative frames for segmentation. Later, the trajectories of centroids and lowest points of the segmented pelvic organs were modeled using a CSHMM to classify the severity of POP. Results demonstrate that the proposed method can accurately track and segment the pelvic organs and improve the classification of the severity of pelvic prolapse by modeling the resulted trajectories. The proposed method can be used to quantitatively analyze the movement of pelvic organs on MRI to improve understanding of POP, complement clinical examination, and possibly improve treatment and outcomes. It can also be used for the automatic tracking, segmentation, and classification of deformable structures from a sequence of images. As future work, we plan to collect additional data to perform experiments on a larger dataset and extend this work for the classification of all the five stages of POP.

Disclosures

Authors I. Nekooeimehr, S. Lai-Yuen, P. Bao, and A. Weitzenfeld report no conflicts of interest. S. Hart reports personal fees from Boston Scientific, Covidien, Cooper Surgical, and Stryker during the conduct of the study.

References

1. P. Dallenbach et al., "Incidence rate and risk factors for vaginal vault prolapse repair after hysterectomy," *Int. Urogynecol. J.* **19**(12), 1623–1629 (2008).
2. L. L. Subak et al., "Cost of pelvic organ prolapse surgery in the United States," *Obstet. Gynecol.* **98**, 646–651 (2001).
3. J. R. Popovic and L. J. Kozak, "National hospital discharge survey: annual summary, 1998," *Vital Health Stat.* **13**, 1–194 (2000).
4. C. Persu et al., "Pelvic organ prolapse quantification system (POP–Q)—a new era in pelvic prolapse staging," *J. Med. Life* **4**, 75–81 (2011).
5. K. Singh, W. M. Reid, and L. A. Berger, "Assessment and grading of pelvic organ prolapse by use of dynamic magnetic resonance imaging," *Am. J. Obstet. Gynecol.* **185**(1), 71–77 (2001).
6. B. Vakili et al., "Levator contraction strength and genital hiatus as risk factors for recurrent pelvic organ prolapse," *Am. J. Obstet. Gynecol.* **192**(5), 1592–1598 (2005).
7. E. Cortes et al., "Clinical examination and dynamic magnetic resonance imaging in vaginal vault prolapse," *Obstet. Gynecol.* **103**, 41–46 (2004).
8. A. Lienemann et al., "Assessment of pelvic organ descent by use of functional cine-MRI: which reference line should be used?" *Neurourol. Urodyn.* **23**, 33–37 (2004).
9. C. J. Robinson et al., "Prediction of pelvic organ prolapse using an artificial neural network," *Am. J. Obstet. Gynecol.* **199**, 193.e1–193.e6 (2008).
10. S. Onal et al., "MRI based segmentation of pubic bone for evaluation of pelvic organ prolapse," *IEEE J. Biomed. Health Inf.* **18**(4), 1370–1378 (2014).
11. M. Borse, S. Patil, and B. Patil, "Literature survey for 3D reconstruction of brain MRI images," *Int. J. Res. Eng. Technol.* **2**(11), 743–748 (2013).
12. S. R. Broekhuis et al., "A systematic review of clinical studies on dynamic magnetic resonance imaging of pelvic organ prolapse: the use of reference lines and anatomical landmarks," *Int. Urogynecol. J. Pelvic Floor Dysfunct.* **20**, 721–729 (2009).
13. C. V. Comiter et al., "Grading pelvic prolapse and pelvic floor relaxation using magnetic resonance imaging," *Urology* **54**, 454–457 (1999).
14. M. Rahim et al., "Pelvic organs dynamic feature analysis for MRI sequence discrimination," in *20th Int. Conf. on Pattern Recognition (ICPR)*, pp. 2496–2499 (2010).
15. Z.-W. Chen et al., "Female patient-specific finite element modeling of pelvic organ prolapse (POP)," *J. Biomech.* **48**(2), 238–245 (2015).
16. A. Yilmaz, O. Javed, and M. Shah, "Object tracking: a survey," *ACM Comput. Surv.* **38**(4), 13 (2006).
17. F. Porikli and A. Yilmaz, "Object detection and tracking," in *Video Analytics for Business Intelligence*, C. Shan et al., Eds., Vol. **409**, pp. 3–41, Springer, Berlin, Heidelberg (2012).

18. J. Wang and M. F. Cohen, "Image and video matting: a survey," *Found. Trends Comput. Graphics Vision* **3**(2), 97–175 (2008).
19. B. T. Morris and M. M. Trivedi, "A survey of vision-based trajectory learning and analysis for surveillance," *IEEE Trans. Circuits Syst. Video Technol.* **18**(8), 1114–1127 (2008).
20. J. K. Aggarwal and M. S. Ryoo, "Human activity analysis: a review," *ACM Comput. Surv.* **43**(3), 16 (2011).
21. H. Ardö, K. Åström, and R. Berthilsson, "Online Viterbi optimisation for simple event detection in video," in *International Computer Vision Summer School* (2007).
22. S. Gong and T. Xiang, "Recognition of group activities using dynamic probabilistic networks," in *Ninth IEEE Int. Conf. on Computer Vision, Proc.*, pp. 742–749 (2003).
23. C. Vogler and D. Metaxas, "A framework for recognizing the simultaneous aspects of American Sign Language," *Comput. Vision Image Understanding* **81**(3), 358–384 (2001).
24. X. Ma, D. Schonfeld, and A. Khokhar, "Distributed multi-dimensional hidden Markov model: theory and application in multiple-object trajectory classification and recognition," *Proc. SPIE* **6820**, 68200O (2008).
25. S. Bauer et al., "A survey of MRI-based medical image analysis for brain tumor studies," *Phys. Med. Biol.* **58**(13), R97–R129 (2013).
26. H. Wang and A. Amini, "Cardiac motion and deformation recovery from MRI: a review," *IEEE Trans. Med. Imaging* **31**(2), 487–503 (2012).
27. Y. Zhang et al., "Dynamic lung modeling and tumor tracking using deformable image registration and geometric smoothing," in *Computational Modelling of Objects Represented in Images III: Fundamentals, Methods and Applications*, L. Di Giamberardino et al., Eds., pp. 215–220, Taylor & Francis Group, London (2012).
28. M. Rahim et al., "A diffeomorphic mapping based characterization of temporal sequences: application to the pelvic organ dynamics assessment," *J. Math. Imaging Vision* **47**(1–2), 151–164 (2013).
29. M. Cosson et al., "Simulation of normal pelvic mobilities in building an MRI-validated biomechanical model," *Int. Urogynecol. J.* **24**(1), 105–112 (2013).
30. M. Parente et al., "Deformation of the pelvic floor muscles during a vaginal delivery," *Int. Urogynecol. J.* **19**(1), 65–71 (2008).
31. J. C. Nascimento, M. A. Figueiredo, and J. S. Marques, "Trajectory classification using switched dynamical hidden Markov models," *IEEE Trans. Image Process.* **19**(5), 1338–1348 (2010).
32. F. E. Grubbs, "Procedures for detecting outlying observations in samples," *Technometrics* **11**(1), 1–21 (1969).
33. T. F. Chan and L. A. Vese, "Active contours without edges," *IEEE Trans. Image Process.* **10**(2), 266–277 (2001).
34. G. D. Forney, Jr., "The Viterbi algorithm," *Proc. IEEE* **61**(3), 268–278 (1973).
35. M. P. Sampat et al., "Complex wavelet structural similarity: a new image similarity index," *IEEE Trans. Image Process.* **18**(11), 2385–2401 (2009).
36. D. P. Huttenlocher, G. A. Klanderman, and W. J. Rucklidge, "Comparing images using the Hausdorff distance," *IEEE Trans. Pattern Anal. Mach. Intell.* **15**(9), 850–863 (1993).
37. C. A. Woodfield et al., "Magnetic resonance imaging of pelvic organ prolapse: comparing pubococcygeal and midpubic lines with clinical staging," *Int. Urogynecol. J.* **20**(6), 695–701 (2009).

Iman Nekooeimehr is an operations research consultant at Revenue Analytics. He received his BS degree in industrial engineering from Sharif University of Technology in 2011 and his MS and PhD degrees in industrial engineering from the University of South Florida in 2013 and 2016, respectively. His research interests are in medical image processing, machine learning, and healthcare data analytics.

Susana Lai-Yuen is an associate professor of Industrial and Management Systems Engineering at the University of South Florida, Tampa, Florida, USA. She received her PhD, MS, and BS (summa cum laude) degrees in industrial engineering from North Carolina State University, Raleigh, North Carolina, USA. Her research interests include machine learning, data mining, and product design with applications in medical image processing, computer-aided decision support systems, clinical diagnosis, and medical device design.

Paul Bao was an associate professor in the Department of Computer Science and Engineering, University of South Florida, Tampa, Florida, USA. He received his PhD in computer science from the University of Calgary, Calgary, Alberta, Canada. His research interests include computer graphics and virtual reality, image-based rendering, image/video processing, multimedia systems, and wireless multimedia technologies.

Alfredo Weitzenfeld is a professor in the Department of Computer Science and Engineering, University of South Florida, Tampa, Florida, USA. He received his PhD in computer science and his MS degree in computer engineering from the University of Southern California, Los Angeles, California, USA. He received his BS degree in electrical engineering from the Technion, Haifa, Israel. His main research interests include biologically inspired robotics, neural computational modeling, humanoid robots, and cognitive and multirobot systems.

Stuart Hart is a director of the Global Medical Affairs for Medtronic Surgical Innovations and a voluntary faculty of Obstetrics and Gynecology in the Division of Female Pelvic Medicine and Reconstructive Surgery, University of South Florida, Morsani College of Medicine. He is board-certified in Obstetrics and Gynecology and subspeciality board-certified in female pelvic medicine and reconstructive surgery.